Self-Assembled Monolayers

DOI: 10.1002/ange.201001625

Oligomers and Cyclooligomers of Rigid Phenylene–Ethynylene–Butadiynylenes: Synthesis and Self-Assembled Monolayers**

Stefan-S. Jester, Natalia Shabelina, Stephan M. Le Blanc, and Sigurd Höger**

Nanoscale shape-persistent macrocycles have attracted increasing attention because of their interesting structural, optical, and electronic properties. Moreover, they are able to build up highly organized supramolecular nanostructures in one, two, and three dimensions.[1] Recently, special emphasis has been given to self-assembled monolayers (SAMs) of shape-persistent macrocycles on solid substrates.[2] The ring sizes and distances can be adjusted by the building blocks, and their interior and exterior can synthetically be addressed independently. Together, this allows a surface functionalization with atomic-level precision. In several cases, such patterns could be used for the epitaxial deposition of admolecules.[3]

The driving forces for the self-assembly are the molecule–substrate and molecule–molecule interactions, which are dominated by van der Waals forces. Although rigid macrocycles and rigid linear oligomers[4] have come into the focus of recent scanning tunneling microscopy (STM) studies, a systematic investigation of rigid rods connected by freely jointed or freely rotating linkers[5] and their corresponding closed-loop structures on a solid substrate have been rarely reported, if at all.

In our own ongoing studies, we have prepared arylene–ethynylene–butadiynylene macrocycles with a variety of symmetries, sizes, and functionalities. In most cases, the final ring closure towards our target structures is achieved by an oxidative coupling of rigid bisacetylenes. This transformation typically proceeds by Glaser, Glaser–Eglinton, Hay, or palladium-mediated homocoupling reactions, and has been used numerous times for the formation of macrocyclic structures.[6,7] Oxidative acetylene coupling reactions are easy to perform and tolerate a wide variety of functional groups. Notwithstanding, the actual reaction outcome strongly depends not only on the catalyst/oxidant mixture but also on the solvent and reaction temperature, and of course on the specific substrate structure. Sometimes cyclic and acyclic reaction products are formed simultaneously.[8] In other cases, a catalyst discrimination between different macrocyclic[9] or between acyclic and cyclic reaction products was observed.[10]

Herein, we present a series of acyclic and cyclic phenylene–ethynylene–butadiynylene(PEB) oligomers prepared by oxidative acetylene oligomerization. These oligomers are based on the same constitutional repeating units (CRUs), in which the rigid elements of the target structures are connected by freely rotating linkers bearing pyridyl functions.[11] Our study was motivated by the question as to whether these oligomers can form stable SAMs at the solid/liquid interface that can be investigated by STM. We wanted to determine the behavior of oligomers of different length and compare directly acyclic and cyclic structures, a topic that has not yet been addressed.

The synthesis of the precursors (half-rings) **1a** and **4a** is described in the Supporting Information. They were coupled using CuCl/TMEDA (1:1)[12] as catalyst and base, air oxygen as oxidant, and dichloromethane as solvent (Scheme 1, left).[13] Analytical gel permeation chromatography (GPC) of the crude product indicated the formation of dimers along with higher oligomers (see Figure 2 A (a)). Similarly, the palladium-catalyzed oxidative acetylene coupling of **1a** and **1b** and of **4a** and **4b** using $[Pd(PPh_3)_2Cl_2]$ and CuI as catalysts, I_2 as oxidant, and iPr_2NH as base in THF as solvent (Scheme 1, right) produced again an oligomer mixture. However, the peak molecular weights of the oligomers were significantly lower (see Figure 2 B (a)).

Recycling GPC (recGPC) allowed an efficient separation and detailed analysis of the different products. From the copper-catalyzed coupling of **4a**, we separated acyclic oligomers $[\mathbf{5a}]_n$ from the dimer ($n=2$) up to the hexamer ($n=6$) in yields between 15 % and 4 %;[14] from the palladium-catalyzed coupling, cyclic oligomers $[\mathbf{6a}]_n$ from the dimer ($n=2$) to the hexamer ($n=6$) were obtained in yields between 19 % and 2 %.[15] From the copper-promoted coupling reaction of **1a**, we isolated the acyclic oligomers ($[\mathbf{2a}]_n$; $n=2$–6) in yields between 22 % and 6 %. Under palladium catalysis, both **1a** and **1b** only gave cyclodimers $[\mathbf{3a}]_2$ and $[\mathbf{3b}]_2$; higher oligomers show the presence of defects (Supporting Information).[16–18] However, the pure acyclic and the cyclic oligomers are slightly yellow and show a strong blue fluorescence in solution.

With oligomers $[\mathbf{5a}]_n$ and $[\mathbf{6a}]_n$ ($n=2$–6) now available, we were able to systematically investigate not only the adsorption behavior of defined, monodisperse oligomers of different lengths (and compare them with the monomer, **4a**), but could also directly compare cyclic and acyclic compounds of the same chain length. An STM image of the monomer adsorbed at the interface of highly oriented pyrolytic graphite (HOPG)/1,2,4-trichlorobenzene (TCB) is shown in Figure 1 a,

[*] Dr. S.-S. Jester, Dr. N. Shabelina, S. M. Le Blanc, Prof. Dr. S. Höger
Kekulé-Institut für Organische Chemie und Biochemie
Rheinische Friedrich-Wilhelms-Universität Bonn
Gerhard-Domagk-Strasse 1, 53121 Bonn (Germany)
Fax: (+49) 228-73-5662
E-mail: stefan.jester@uni-bonn.de
hoeger@uni-bonn.de

[**] Financial support by the DFG, the SFB 624, and the Volkswagen-Stiftung is gratefully acknowledged.

Supporting information for this article is available on the WWW under http://dx.doi.org/10.1002/anie.201001625.

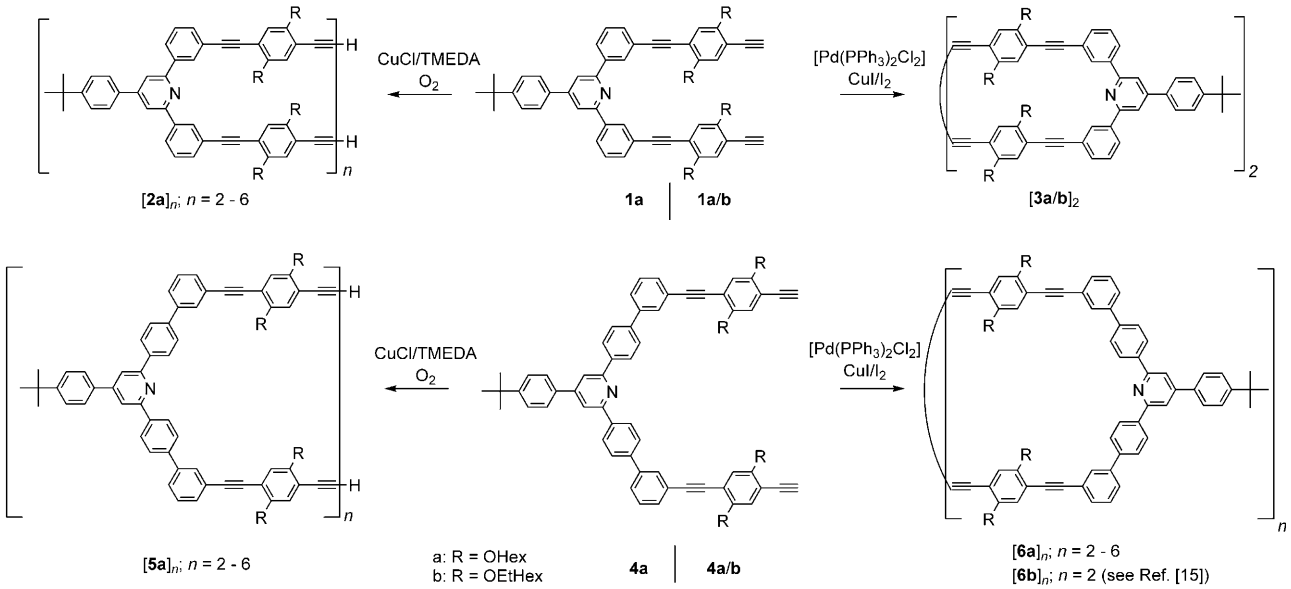

Scheme 1. Oxidative acetylene coupling of **1a/b** and **4a/b**. TMEDA = *N*,*N*,*N*′,*N*′-tetramethylethylenediamine, OEtHex = 2-ethylhexyloxy.

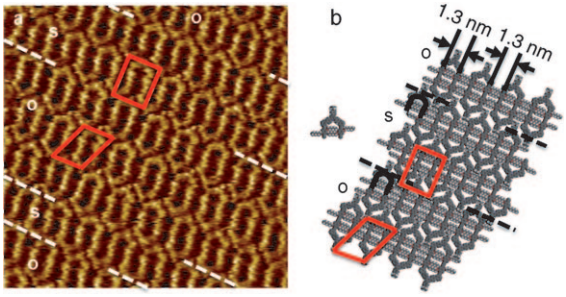

Figure 1. a) STM image of **4a** at the solid/liquid interface between highly oriented pyrolytic graphite (HOPG) and 1,2,4-trichlorobenzene (TCB). b) Molecular model of the SAM of **4a** (see also Ref. [21]). The unit cells of the O- and S-shaped polymorphs are shown in red.

and STM images of the acyclic and cyclic oligomers are shown in Figure 2 A,B (b–f). Bright and dark colors indicate local high and low tunneling currents resulting from unsaturated (backbone) and saturated (alkoxy side chain) hydrocarbon segments, respectively.[19]

For the monomer **4a** (Figure 1 a) and the acyclic dimer $[\mathbf{5a}]_2$ (Figure 2 A (b)), O- and S-shaped polymorphs are observed concurrently, while for the higher ($n > 2$) acyclic oligomers, solely S-shaped geometries are adopted. The backbone distances in lamellar alignments of linear oligo-PE(B)s are determined by the alkyl/alkoxy substituent chain lengths,[4] and the corner units of **4a** and $[\mathbf{5a}]_{2-6}$ perfectly match the expected distances for hexyloxy-substituted oligo-PEBs.[4f] The intramolecular and intermolecular rod–rod distances (1.3 nm) cannot be distinguished at the experimental resolution. This is also strongly supported by the models in Figure 1 b and 2 A,B (b–f).

The acetylene ends of adjacent molecules point to each other, and the kinks form densely packed structures. The sinuous adsorbates interlock in such a way that rectangular unit cells can be indexed. In the case of packing errors and domain boundaries of the S-shaped adsorbate rows, the (ethynyl terminated) open ends of the acyclic oligomers can be discerned (as marked by white arrows in Figure 2 A (d–f)), and individual molecules are distinguishable.[20] Alternatively, one might also expect W-shaped adsorbate geometries (see Supporting Information). However, such pattern motifs were not observed. At present, we assume that the commensurability of the alkyl chains with the HOPG substrate would cause unfavorable strain in the backbone.

Whilst open-chain oligomers can easily adopt S-shaped geometries and therefore pack closely on the HOPG/TCB interface, the texturing behavior of the corresponding macrocycles is, apart from the shape-persistent compound $[\mathbf{6a}]_2$, hardly predictable. $[\mathbf{6a}]_2$ forms rows of densely packed rings, and the structure is indistinguishable from the O-shaped polymorph of $[\mathbf{5a}]_2$. The higher macrocycles formed by an even number of monomers, $[\mathbf{6a}]_4$ and $[\mathbf{6a}]_6$, adopt an elongated collapsed conformation. Two of the *meta*-substituted corner segments form the short sides of a quasi-rectangular structure, while the other two (four in $[\mathbf{6a}]_6$) are integrated into the long sides of the latter. This allows a dense packing of the compounds at the interface. Again, in all cases the distance between the opposite long sides of the molecule (1.3 nm) is indistinguishable within experimental error from the intermolecular distance between two macrocycles (1.3 nm). An open (less-dense) adsorbate conformation (Supporting Information), in which the macrocycles have large cavities, is in not observed in any of the cases. The macrocycles formed by an uneven number of monomers cannot assemble into comparably dense structures. Compound $[\mathbf{6a}]_3$ forms mushroom-shaped adsorbates organized into ordered double rows (for details see the Supporting Information). However, for $[\mathbf{6a}]_5$ (though treated similarly), no two-dimensional crystallization could be observed. The molecules adopt a larger variety of conformations, although

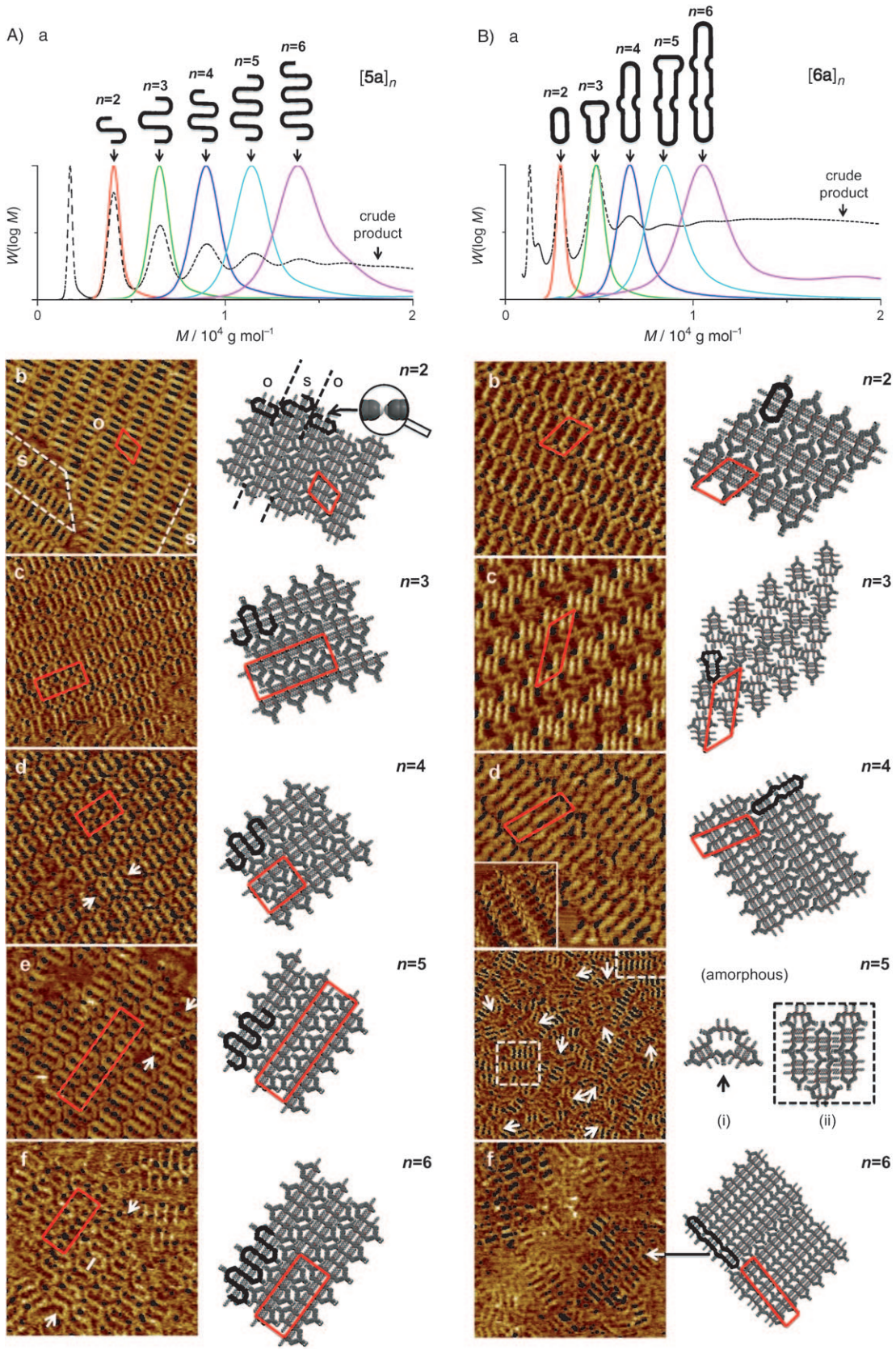

Figure 2. a) Superposed analytical GPC elugrams of the product mixtures of [**5a**]$_n$ from the copper-catalyzed reaction (A) and [**6a**]$_n$ from the palladium-catalyzed reaction (B) before (----) and after (——) preparative recGPC separation. Colors indicate the oligomers of different lengths: $n = 2$–6. b)–f) STM images of self-assembled monolayers of the separated oligomers at the solid(HOPG)/liquid(TCB) interface. For each STM image, the corresponding molecular model is shown.[22] (Further details, such as image and unit cell dimensions, are given in Ref. [24]; additional images are shown in the Supporting Information.)

conformer (i) of $[\mathbf{6a}]_5$ is repeatedly observed (Figure 2B(e), arrows), and more elongated shapes (for example (ii), indicated by dashed boxes) are also found. Structure (i) can be constructed from two mushroom-shaped structures $[\mathbf{6a}]_3$ that share the mushroom cap, whereas structures in (ii) can be viewed as a combination of structures $[\mathbf{6a}]_3$ and $[\mathbf{6a}]_4$. The molecules do not pack into a large regular ordered lattice.

Our STM investigations have revealed a general difference in the adsorption behavior of the acyclic and cyclic oligomer series $[\mathbf{5a}]_n$ and $[\mathbf{6a}]_n$ ($n = 2$–6), respectively. The structures of the SAMs of the acyclic oligomers (freely rotating chains) are determined by the kinks and alkoxy substituents, and by the shape complementarity of the resulting sinuous patterns. In contrast, the structures of the macrocycle patterns are strongly size-dependent. Although patterns of cycles formed from an even number ($n = 2, 4, 6$) of monomers follow a common conformation principle, trimers construct a unique and unexpected molecular grid, and pentamer films are amorphous.

Although STM studies on shape-persistent macrocycles are currently a topic of high interest, the exploration of higher (and more flexible) oligomers is still in its infancy. Currently, we investigate how general these observed structural motifs are and whether compounds of analogous structures will adopt similar conformations.

Received: March 18, 2010
Revised: May 4, 2010
Published online: July 20, 2010

Keywords: gel-permeation chromatography · Glaser coupling · macrocycles · scanning probe microscopy · self-assembled monolayers

[1] a) J. S. Moore, *Acc. Chem. Res.* **1997**, *30*, 402; b) S. Höger, *J. Polym. Sci. Part A* **1999**, *37*, 2685; c) C. Grave, A. D. Schlüter, *Eur. J. Org. Chem.* **2002**, 3075; d) Y. Yamaguchi, Z. Yoshida, *Chem. Eur. J.* **2003**, *9*, 5430; e) J. A. Marsden, G. J. Palmer, M. M. Haley, *Eur. J. Org. Chem.* **2003**, 2355; f) S. Höger, *Angew. Chem.* **2005**, *117*, 3872; *Angew. Chem. Int. Ed.* **2005**, *44*, 3806; g) W. Zhang, J. S. Moore, *Angew. Chem.* **2006**, *118*, 4524; *Angew. Chem. Int. Ed.* **2006**, *45*, 4416.

[2] a) S. Höger, K. Bonrad, A. Mourran, U. Beginn, M. Möller, *J. Am. Chem. Soc.* **2001**, *123*, 5651; b) D. Borissov, A. Ziegler, S. Höger, W. Freyland, *Langmuir* **2004**, *20*, 2781; c) K. Tahara, C. A. Johnson II, T. Fujita, M. Sonoda, F. C. de Schryver, S. de Feyter, M. M. Haley, Y. Tobe, *Langmuir* **2007**, *23*, 10190; d) S. Lei, K. Tahara, F. C. de Schryver, M. van der Auweraer, Y. Tobe, S. de Feyter, *Angew. Chem.* **2008**, *120*, 3006; *Angew. Chem. Int. Ed.* **2008**, *47*, 2964.

[3] a) G.-B. Pan, X.-H. Cheng, S. Höger, W. Freyland, *J. Am. Chem. Soc.* **2006**, *128*, 4218; b) E. Mena-Osteritz, P. Bäuerle, *Adv. Mater.* **2006**, *18*, 447; c) S. Furukawa, K. Tahara, F. C. de Schryver, M. van der Auweraer, Y. Tobe, S. de Feyter, *Angew. Chem.* **2007**, *119*, 2889; *Angew. Chem. Int. Ed.* **2007**, *46*, 2831; d) K. Tahara, S. Lei, D. Mössinger, H. Kozuma, K. Inukai, M. Van der Auweraer, F. C. de Schryver, S. Höger, Y. Tobe, S. de Feyter, *Chem. Commun.* **2008**, 3897; e) K. Tahara, S. Lei, W. Mamdouh, Y. Yamaguchi, T. Ichikawa, H. Uji-i, M. Sonoda, K. Kirose, F. C. de Schryver, S. de Feyter, Y. Tobe, *J. Am. Chem. Soc.* **2008**, *130*, 6666; f) S. Lei, K. Tahara, X. Feng, S. Furukawa, F. C. de Schryver, K. Müllen, Y. Tobe, S. De Feyter, *J. Am. Chem. Soc.* **2008**, *130*, 7119; g) B. Schmaltz, A. Rouhanipour, H. J. Räder, W. Pisula, K. Müllen, *Angew. Chem.* **2009**, *121*, 734; *Angew. Chem. Int. Ed.* **2009**, *48*, 720; h) J. Adisoejoso, K. Tahara, S. Okuhata, S. Lei, Y. Tobe, S. de Feyter, *Angew. Chem.* **2009**, *121*, 7489; *Angew. Chem. Int. Ed.* **2009**, *48*, 7353; i) T. Chen, G.-B. Pan, H. Wettach, M. Fritzsche, S. Höger, L.-J. Wan, H.-B. Yang, B. H. Northrop, P. J. Stang, *J. Am. Chem. Soc.* **2010**, *132*, 1328.

[4] For recent publications about SAMs of shape-persistent linear coupling products see, e.g.: a) P. Samorí, N. Severin, K. Müllen, J. P. Rabe, *Adv. Mater.* **2000**, *12*, 579; b) J.-R. Gong, J.-L. Zhao, S.-B. Lei, L.-J. Wan, Z.-S. Bo, X.-L. Fan, C.-L. Bai, *Langmuir* **2003**, *19*, 10128; c) Z. Mu, X. Yang, Z. Wang, X. Zhang, *Langmuir* **2004**, *20*, 8892; d) Z.-Y. Yang, L.-H. Gan, S.-B. Lei, L.-J. Wan, C. Wang, J.-Z. Jiang, *J. Phys. Chem. B* **2005**, *109*, 19859; e) J.-R. Gong, H.-J. Yan, Q.-H. Yuan, L.-P. Xu, Z.-S. Bo, L.-J. Wan, *J. Am. Chem. Soc.* **2006**, *128*, 12384; f) K. Yoosaf, P. V. James, A. R. Ramesh, C. H. Suresh, K. G. Thomas, *J. Phys. Chem. C* **2007**, *111*, 14933; g) M. Wielopolski, A. Atienza, T. Clark, D. M. Guldi, N. Martín, *Chem. Eur. J.* **2008**, *14*, 6379; h) D. Mössinger, S.-S. Jester, E. Sigmund, U. Müller, S. Höger, *Macromolecules* **2009**, *42*, 7974.

[5] Freely jointed chains are rigid segments of fixed length, interconnected by linkers that allow variable valence angles and rotation. In contrast, the hinges of freely rotating chains enforce fixed angles between adjacent segments, whilst still allowing free rotation with all torsion angles being equally likely. After adsorption to the substrate, the rotation is restricted, and the linked units may adopt cisoidal and transoidal conformation.

[6] a) C. Glaser, *Ber. Dtsch. Chem. Ges.* **1869**, *2*, 422; b) G. Eglinton, A. R. Galbraith, *Proc. Chem. Soc.* **1957**, 350; c) O. M. Behr, G. Eglinton, A. R. Galbraith, R. A. Raphael, *J. Chem. Soc.* **1960**, 3614; d) A. S. Hay, *J. Org. Chem.* **1962**, *27*, 3320; e) R. Rossi, A. Carpita, C. Bigelli, *Tetrahedron Lett.* **1985**, *26*, 523; f) P. Siemsen, R. C. Livingston, F. Diederich, *Angew. Chem.* **2000**, *112*, 2740; *Angew. Chem. Int. Ed.* **2000**, *39*, 2632.

[7] a) F. Sondheimer, R. Wolovsky, *J. Am. Chem. Soc.* **1962**, *84*, 260; b) F. Sondheimer, *Acc. Chem. Res.* **1972**, *3*, 81; c) D. O'Krongly, S. R. Denmeade, M. Y. Chiang, R. Breslow, *J. Am. Chem. Soc.* **1985**, *107*, 5544; d) K. Kadei, F. Vögtle, *Chem. Ber.* **1991**, *124*, 909.

[8] A. de Meijere, S. Kozhushkov, T. Haumann, R. Boese, C. Puls, M. J. Cooney, L. T. Scott, *Chem. Eur. J.* **1995**, *1*, 124.

[9] J. A. Marsden, J. J. Miller, M. M. Haley, *Angew. Chem.* **2004**, *116*, 1726; *Angew. Chem. Int. Ed.* **2004**, *43*, 1694.

[10] Tobe could specifically couple bisacetylenes to form the acyclic oligomers under Hay conditions, whereas cyclic oligomers were formed under Eglinton contitions; see: Y. Tobe, N. Utsumi, A. Nagano, M. Sonoda, K. Naemura, *Tetrahedron* **2001**, *57*, 8075.

[11] For pyridyl-containing rigid macrocycles, see for example: a) Y. Tobe, A. Nagano, K. Kawabata, M. Sonoda, K. Naemura, *Org. Lett.* **2000**, *2*, 3265; b) S.-S. Sun, A. J. Lees, *Organometallics* **2001**, *20*, 2353; c) K. Campbell, R. McDonald, R. R. Tykwinski, *J. Org. Chem.* **2002**, *67*, 1133; d) O. Henze, D. Lentz, A. Schäfer, P. Franke, A. D. Schlüter, *Chem. Eur. J.* **2002**, *8*, 357; e) M. Schmittel, H. Ammon, V. Kalsani, A. Wiegrefe, C. Michel, *Chem. Commun.* **2002**, 2566; f) P. N. W. Baxter, *Chem. Eur. J.* **2003**, *9*, 5011; g) Y. Yamaguchi, Z.-i. Yoshida, *Chem. Eur. J.* **2003**, *9*, 5430; h) C. Grave, D. Lentz, A. Schäfer, P. Samorì, J. P. Rabe, P. Franke, A. D. Schlüter, *J. Am. Chem. Soc.* **2003**, *125*, 6907.

[12] The ratio of TMEDA to CuCl is of high importance for the reaction. With an excess of TMEDA, halogenation of the acetylenes was observed (see Supporting Information); see also: T. Hamada, X. Ye, S. S. Stahl, *J. Am. Chem. Soc.* **2008**, *130*, 833.

[13] Attempts to couple **1a** or **4a** under pseudo-high-dilution conditions using $CuCl/CuCl_2$ as catalyst/oxidant mixture and pyridine as solvent were not successful, and only a dark brown

tarry material of unknown composition could be isolated. The absence of cyclodimers was surprising, as the same coupling conditions worked well in most of our acetylene coupling reactions and gave (with a similar but smaller substrate) high to nearly quantitative product yields; see: N. Shabelina, S. Klyatskaya, V. Enkelmann, S. Höger, *C. R. Chim.* **2009**, *12*, 430. Opris et al. also obtained cyclic products when bipyridyl containing bis(acetylene)s were oxidatively coupled under copper catalysis: D. M. Opris, A. Ossenbach, D. Lentz, A. D. Schlüter, *Org. Lett.* **2008**, *10*, 2091. Similarly, Kim et al. obtained rectangular shape-persistent macrocycles under copper catalysis; see: J.-K. Kim, E. Lee, M.-C. Kim, E. Sim, M. Lee, *J. Am. Chem. Soc.* **2009**, *131*, 17768.

[14] **1b** and **4b** were not investigated under the conditions of the copper-catalyzed reaction.

[15] Only the cyclodimer $[\mathbf{6b}]_2$ was identified when **4b** was coupled under palladium catalysis; higher oligomers were not characterized.

[16] Considering **1b** and **4b** with 2-ethylhexyloxy side chains, solubility is clearly not responsible for the observed discrimination between cyclic and acyclic products.

[17] Proton NMR studies (see Supporting Information) showed that all oligomers obtained from the copper-promoted coupling reactions still contain ethynyl end groups, whereas all separated fractions of the palladium-catalyzed coupling reactions did not exhibit ethynyl protons. Furthermore, the peak patterns of the aromatic protons in the spectra are different for both reactions. HRMS data for $[\mathbf{5a}]_2$ and $[\mathbf{6a}]_2$ show the exact masses for the proposed structures.

[18] The difference in conformational freedom between the acyclic and cyclic oligomers is also reflected by their thermal behavior. Although the acyclic dimers $[\mathbf{2a}]_2$ and $[\mathbf{5a}]_2$ have melting points of 71 °C and 95 °C, the cyclic analogue $[\mathbf{3a}]_2$ melts at 221 °C and $[\mathbf{6a}]_2$ decomposes at >325 °C; see: H. A. Staab, H. Bräumling, K. Schneider, *Chem. Ber.* **1968**, *101*, 879, and Ref. [10].

[19] For theoretical descriptions of the contrast mechanism in STM, see for example: a) R. Lazzaroni, A. Calderone, J. L. Brédas, J. P. Rabe, *J. Chem. Phys.* **1997**, *107*, 99; b) P. Sautet, *Chem. Rev.* **1997**, *97*, 1097.

[20] As visualized by the inset of the molecular model in Figure 2A(b), the distance of the terminal ethynyl units is smaller than the lateral changes of the tunneling current. Therefore, we cannot clearly resolve the difference of the cyclic and acyclic dimer, $[\mathbf{5a}]_2$ and $[\mathbf{6a}]_2$, by microscopy. Nevertheless, the presence of a cyclic dimer $[\mathbf{6a}]_2$ as impurity in $[\mathbf{5a}]_2$ could be excluded by GPC, HRMS, and ^{1}H NMR analysis.[17] Furthermore, the presence of two distinguishable O- and S-shaped polymorphs of the dimer $[\mathbf{14a}]_2$ on HOPG is rather expected instead of peculiar.

[21] STM image size, tunneling parameters, concentration, and unit cell dimensions for the SAM of the monomer **4a** on HOPG are: 24.1×24.1 nm^2, $V_s=-0.95$ V, $I_t=6$ pA, $c=10^{-4}$ mol L^{-1}; O-shaped polymorph: $a=3.8\pm0.1$ nm, $b=2.7\pm0.1$ nm, $\gamma=68\pm2°$; S-shaped polymorph: $a=3.6\pm0.1$ nm, $b=2.7\pm0.1$ nm, $\gamma=90\pm2°$.

[22] In Figure 1, Figure A2(b–f), and Figure 2B(b,d), the unit cell vectors along the lamellar directions are oriented with $9\pm2°$ towards the main axis of the HOPG substrate (see Supporting Information), indicating surface induced chirality of the molecules. For the alkoxy substituents, we assume the common commensurability of *all-gauche*-constituted alkyl chains on the graphene surface lattice.[23] We conclude that the angle between the rigid PEB rods and the alkyl chains must be $81\pm2°$ for the considered systems $[\mathbf{5a}]_n$ and $[\mathbf{6a}]_n$. Clearly, this angle is not a generally constant value for all alkoxy-substituted rigid systems, but will rather strongly depend on the concrete PEB backbone sequence. However, as individual short alkoxy chains (such as OC_6H_{13} in this case) cannot be resolved by STM under the applied conditions, their orientation shall not be further discussed herein.

[23] For SAMs of alkanes on HOPG, see for example: T. Yang, S. Berber, J.-F. Liu, G. P. Miller, D. Tománek, *J. Chem. Phys.* **2008**, *128*, 124709, and references therein.

[24] The sizes of the STM images, tunneling parameters, applied solutions, and annealing temperatures, and the dimensions of the unit cells of the self-assembled monolayers of acyclic oligomers $[\mathbf{5a}]_{2\text{–}6}$ are as follows: b) dimer $[\mathbf{5a}]_2$ (34.0×34.0 nm^2, $V_s=-1.1$ V, $I_t=150$ pA, $c=10^{-5}$ mol L^{-1}, unit cell: $a=3.9\pm0.1$ nm, $b=2.7\pm0.1$ nm, $\gamma=68\pm2°$); c) trimer $[\mathbf{5a}]_3$ (32.4×32.4 nm^2, $V_s=-1.35$ V, $I_t=100$ pA, $c=10^{-5}$ mol L^{-1}, annealed to 60 °C for 2 min, unit cell: $a=8.2\pm0.2$ nm, $b=3.8\pm0.1$ nm, $\gamma=90\pm2°$); d) tetramer $[\mathbf{5a}]_4$ (28.0×28.0 nm^2, $V_s=-1.1$ V, $I_t=120$ pA, $c=10^{-6}$ mol L^{-1}, annealed to 80 °C for 2 min, unit cell: $a=5.4\pm0.2$ nm, $b=3.8\pm0.1$ nm, $\gamma=90\pm2°$); e) pentamer $[\mathbf{5a}]_5$ (24.3×24.3 nm^2, $V_s=-0.85$ V, $I_t=11$ pA, $c=10^{-5}$ mol L^{-1}, annealed to 80 °C for 2 min, unit cell: $a=13.5\pm0.2$ nm, $b=3.8\pm0.1$ nm, $\gamma=90\pm2°$); f) hexamer $[\mathbf{5a}]_6$ (25.3×25.3 nm^2, $V_s=-0.3$ V, $I_t=246$ pA, $c=10^{-5}$ mol L^{-1}, annealed to 80 °C for 2 min, unit cell: $a=8.0\pm0.2$ nm, $b=3.8\pm0.1$ nm, $\gamma=90\pm2°$). The respective parameter sets for cyclic oligomers $[\mathbf{6a}]_{2\text{-}6}$: b) dimer $[\mathbf{6a}]_2$ (20.9×20.9 nm^2, $V_s=-0.42$ V, $I_t=14$ pA, $c=10^{-5}$ M, unit cell: $a=3.8\pm0.1$ nm, $b=2.7\pm0.1$ nm, $\gamma=69\pm2°$); c) trimer $[\mathbf{6a}]_3$ (30.8×30.8 nm^2, $V_s=-1.1$ V, $I_t=5$ pA, $c=10^{-6}$ mol L^{-1}, annealed to 80 °C for 2 min, unit cell: $a=10.1\pm0.2$ nm, $b=4.7\pm0.1$ nm, $\gamma=44\pm2°$); d) tetramer $[\mathbf{6a}]_4$ (26.0×26.0 nm^2, $V_s=-1.43$ V, $I_t=14$ pA, $c=10^{-5}$ mol L^{-1}, annealed to 80 °C for 2 min, inset: 12.1×12.1 nm^2, $V_s=-1.20$ V, $I_t=10$ pA, unit cell: $a=7.6\pm0.2$ nm, $b=2.7\pm0.1$ nm, $\gamma=79\pm3°$); e) pentamer $[\mathbf{6a}]_5$ (50×50 nm^2, $V_s=-0.87$ V, $I_t=43$ pA, $c=10^{-5}$ mol L^{-1}, annealed to 80 °C for 2 min, amorphous); f) hexamer $[\mathbf{6a}]_6$ (40×40 nm^2, $V_s=-0.6$ V, $I_t=14$ pA, $c=10^{-5}$ mol L^{-1}, annealed to 80 °C for 2 min, expected unit cell: $a=11.5$ nm, $b=2.7$ nm, $\gamma=83°$). Note: a and b denote the long and short unit cell vectors, respectively. By definition, the unit cells for (sufficiently large) odd acyclic oligomers $[\mathbf{5a}]_n$ ($n=3, 5$) are larger than for the respective even oligomers ($n=4, 6$). All images were calibrated in situ using the HOPG substrate as reference grid (see the Supporting Information).

